Poultry Science

Dynamic changes in the skin transcriptome for the melanin pigmentation in embryonic chickens

Dong Leng,[*,†,1] Maosen Yang,[‖,†,1] Xiaomeng Miao,[‡,1] Zhiying Huang,[¶,†] Mengmeng Li,[†] Jia Liu,[§] Tao Wang,[†] Diyan Li,[†] and Chungang Feng [*,2]

[*]*College of Animal Science and Technology, Nanjing Agricultural University, Nanjing 210095, China;* [†]*School of Pharmacy, Chengdu University, Chengdu 610106, China;* [‡]*Institute of Animal Husbandry and Veterinary Medicine, Guizhou Academy of Agricultural Sciences, Guiyang 550005, China;* [§]*Guizhou Province Livestock and Poultry Genetic Resources Management Station, Guizhou Provincial Department of Agriculture and Rural Affairs, Guiyang 550001, China;* [‖]*College of Animal Science and Technology, Guangxi University, Nanning 530004, China; and* [¶]*College of Animal Science, Shanxi Agricultural University, Taiyuan 030031, China*

ABSTRACT Dermal hyperpigmentation stands out among the various skin pigmentation phenotypes in chickens, where most other pigmentation variants affect feather color and patterning predominantly. Despite numerous black chicken breeds worldwide, only a select few exhibit comprehensive black pigmentation, which encompasses the skin, meat, flesh, and bones. The process of skin melanin pigmentation is intricate and develops successively. Historically, research has concentrated primarily on specific developmental points or stages, but fewer studies have examined the entire transcriptome across the timeline of the development of the embryo integument. In our investigation, we undertook the sequencing of chicken embryo skin samples from d 4 to d 13 of incubation. Our results showed that melanoblasts continued to migrate from E4 to the epidermis until E12. Beginning with E6, melanin was synthesized and transferred to epidermal cells and feather follicles in large quantities, and genes such as *DCT, TYR, TYRP1,* and *MITF* played a key role in this process, which is significantly different from that of white-skinned chickens. There were 854 differentially expressed genes between E7 and E8. At this stage, melanocytes formed dendritic forms and transferred melanin to keratinocytes, while the dorsal skin became visibly dark. In addition, *CDH3*, which is a core factor involved in a variety of biological processes, may have an important impact on skin melanin pigmentation. Collectively, our findings unveiled a phased relationship between the canonical pathway and the noncanonical pathway from E4 to E13. These analyses illuminated the gene regulatory mechanism and provided foundational data that pertained to pigmentation in chickens.

Key words: chicken, skin, transcriptome, embryo, melanin pigmentation

2025 Poultry Science 104:104210
https://doi.org/10.1016/j.psj.2024.104210

INTRODUCTION

Embryonic development is a mesmerizing symphony of cellular events that is choreographed with precision to shape the intricate tapestry of life. Among the myriad processes that unfold during this remarkable journey, the development of pigmentation emerges as a captivating phenomenon. Melanin, the pigment responsible for the diverse hues of skin, hair, and eyes, plays a central role in protection from damage by ultraviolet radiation (Lin et al., 2007). The orchestration of melanin pigmentation during embryonic development is a complex process governed by a myriad of molecular players (Slominski et al., 2004); the skin transcriptome serves as a dynamic score that guides the symphony of melanocyte development and pigmentation. The journey of melanin pigmentation commences with the specification and migration of melanocyte precursor cells that originate from the neural crest (Christiansen et al., 2000; Domingues et al., 2020). These multipotent cells embark on a migratory odyssey, and eventually populate various tissues that include the developing skin (Gammill et al., 2003). At the heart of this process lies the microphthalmia-associated transcription factor (**MITF**), which is a master regulator pivotal for melanocyte development (Levy, et al., 2006). MITF orchestrates the expression of a plethora of genes involved in melanin synthesis

Received April 1, 2024.
Accepted August 8, 2024.

[1]These authors contributed equally to this work.

[2]Corresponding author: fengchungang@njau.edu.cn

(Steingrímsson et al., 2004), which include tyrosinase, is the rate-limiting enzyme in melanogenesis (Braasch et al., 2007). Mutations of this gene resulted in a reduction or lack of pigmentation in the coat, inner ear, and eye (Steingrímsson et al., 2003). The dynamic regulation of MITF and its downstream targets within the animal skin transcriptome contributes to the orchestration of melanin pigmentation.

The study of pigmentation in avian species, particularly in chickens, provides a unique window into the intricate molecular mechanisms that govern melanin synthesis and distribution. The pigmentation of chicken skin is a multifaceted phenomenon, which involves a series of dynamic processes that are regulated at the genetic, cellular, and environmental levels. In oriental countries, the black-boned chicken breeds are valuable genetic resources of domestic chickens, and they are an important animal model for the study of melanin pigmentation (Zhu et al., 2014). This is not only due to its tasty meat, but more importantly, its skin, muscle, and internal organs are all rich in melanin (Zi et al., 2023). The wide spectrum of colors of feathers and skin in chickens is attributed primarily to the presence and distribution of 2 main types of melanin: eumelanin, which is responsible for black and brown colors, and pheomelanin, which is responsible for red and yellow hues (Mundy 2005). Activation of the MC1R protein coded by the melanocortin-1 receptor gene (***MC1R***) leads to increased synthesis of black or brown eumelanin. Meanwhile, low MC1R activity generally leads to increased synthesis of red or yellow phaeomelanin (Robbins et al., 1993). In birds, *MC1R* was first cloned from chickens (Takeuchi et al., 1996b), and a point substitution in this gene was identified subsequently to be associated with melanism (Takeuchi et al., 1996a).

The transcriptome, which represents the entire set of RNA molecules in a cell, provides a dynamic snapshot of gene expression patterns. In the context of pigmentation of chicken skin, the transcriptome unveils the orchestrated expression of genes involved in melanogenesis, which is the process of melanin production. A total of 649 known genes were expressed differentially in the skin of the white and black chickens, and 8 known coat-color genes were also expressed in previous studies (*ASIP, TYR, KIT, TYRP1, OCA2, KITLG, MITF,* and *MC1R*) (Zhang et al., 2015). In addition, 56 differentially expressed lncRNAs were identified from the RNA-seq of dorsal skin, and the TCONS_00054154 played a vital role in melanogenesis, as revealed by the combined analysis of lncRNAs and mRNAs (Zhang et al., 2022b). Genes that included *MC1R, DCT, TYRP1, TYR*, and *ASIP* can be used as candidate markers to improve the blackness of a chicken's skin (Khumpeerawat et al., 2021), due to the effect of breed, sex, and age on the expression of these genes.

Fibromelanosis (**FM**) manifests as a profound pigmentation of the dermal layer throughout the entire body, and it creates a distinct dark blue hue when observed through the transparent epidermis (Dorshorst et al., 2011). The term fibromelanosis was introduced to signify the correlation between pigmentation and internal connective tissue, which is prominent in various anatomical structures, such as the trachea, pericardium, blood vessels, muscle, nerve sheaths, gonads, gut mesenteries, and bone periosteum (Faraco et al., 2001; Muroya et al., 2000).

Our previous studies employed genome-wide association studies (**GWAS**) to identify loci associated with skin pigmentation in chickens, and this provided a foundation for targeted breeding strategies (Li et al., 2017; Li et al., 2019). The transcriptomic information acts as a guidebook for poultry breeders, which enables them to make informed decisions that align with their breeding goals. There is a dynamic change of melanosis of skin during embryonic development of chickens. However, the transcriptome changes associated with this melanosis phenotypic change have not been well documented, especially during developmental stages of the embryo.

We used the Panjiang black-bone chicken as a model to explore the dynamic transcriptome changes of the skin. Our research was designed to investigate potential candidate genes associated with melanin pigmentation, and we aimed to unveil the molecular mechanisms that governed the production and accumulation of melanin in chicken skin. The results of this study should establish a crucial theoretical foundation for the selective breeding of chicken breeds that have distinctive, black-boned characteristics.

MATERIALS AND METHODS

Ethics Statement

Ethics approval and consent to participate: The Ethics Committee of Chengdu University (approved ID: YXY20230122) reviewed the experimental protocols carefully and approved this study.

Animals and Sample Collection

We collected fertilized eggs from Panjiang black-bone chickens (*Gallus gallus*) and Youxin Ma chickens, and placed them under uniform incubation conditions. The incubation parameters were maintained at 37.8°C from d 1 to d 13. The humidity level was regulated at 60% to 65% RH, with a 120-min air change cycle that involved a 30-sec air exchange. The incubation process included automated egg turning, which ceased on the 21st d, with an egg turning cycle of 90 min and an egg turning time of 180 s, and 24 h of light. Haunch skin samples were collected promptly from each individual at 10 different time points that spanned embryonic d 4 to d 13 (i.e., E4, E5, E6, E7, E8, E9, E10, E11, E12, and E13), with 6 replicates for each time point. RNA extraction from the skin tissue followed the procedure outlined below.

RNA Extraction and Sequencing

Total RNA was extracted from each individual using 6 biological triplicates for each developmental stage described above, using the Qiagen RNeasy kit. Ribosomal RNA (**rRNA**) was removed with the Epicentre Ribo-Zero rRNA Removal Kit (Epicentre, Madison, WI), following the manufacturer's protocol. A total of 120 libraries was constructed, and we performed paired-end sequencing (2 × 150 bp) using an Illumina HiSeq 2500 platform.

Bioinformatics Analysis of RNA-seq Data

We initiated data preprocessing by eliminating low-quality reads, and we calculated Q20 and Q30 values along with GC content for the refined reads. The resultant clean data were then aligned to the chicken reference genome (GRCg7b) using STAR software (v2.7.6a) (Dobin, et al., 2013). Quantification of gene expression in transcripts per kilobase per million mapped reads (**TPM**) was conducted using Kallisto (v0.44.0) (Bray, et al., 2016). Subsequently, principal component analysis (**PCA**) was performed based on TPM values that used the "factoextra" package (v1.0.7), and Spearman correlation coefficients were computed to construct a correlation heatmap between pairs of samples. Functional annotation enrichment, which encompassed Gene Ontology (**GO**) terms and Kyoto Encyclopedia of Genes and Genomes (**KEGG**) biochemical pathways, was executed using the clusterProfiler package (v4.9.2) (Wu, et al., 2021).

Data and Materials Availability

The transcriptome sequencing data are available through the Sequence Read Archive (Bio Project ID: PRJNA1056484 and PRJNA1129874).

RESULTS

Overview of Transcriptome Dynamics in 10 Skin Developmental Stages

The aim of this study was to gain a comprehensive understanding of the molecular regulatory mechanisms of skin melanin pigmentation during embryonic development in black-boned chickens. To this end, we analyzed the transcriptome dynamics landscape of the dorsal skin at 10 developmental stages using RNA-seq (Figure 1A). We generated 1.36 billion paired-end reads (2 × 150 bp) from RNA-seq, which was equivalent to 409.23 Gb of sequencing data. The average mapping of clean RNA-seq reads to the reference genome (GRCg7b) was 94.95% (range = 93.57−95.99%) (Supplementary Table S1). These results indicated that the sequencing data had a high quality of comparison.

To show the overall pattern of the transcriptome, we performed PCA analysis and Spearman correlation analysis. The results of PCA analysis showed that the 60 samples were clustered separately according to different developmental stages, and they showed a temporally continuous distribution from stage E4 to E13 (Figure 1B). The highest correlation was found among 6 replicate samples from the same developmental stage (Figure 1C). In addition, 1 sample at stage E13 was more distant from the other 5 samples and, by 3-dimensional PCA analysis, we found that the sample at stage E13 showed a clear separation from the other stage samples (Supplementary Figure S1). Therefore, we hypothesized that this was due to observation bias.

Then, we performed 2-by-2 differential expression analyses for the 10 developmental stages and counted the number of differentially expressed genes that were significantly different in each comparison group (adjusted P-value < 0.01 as well as absolute value of $\log_2$FoldChange > 2) (Figure 1D). The 2 adjacent developmental stages possessed the least number of differentially expressed genes between them, and the number of differentially expressed genes between stages increased gradually as development progressed. Interestingly, the number of differential genes between the 2 stages E7 and E8 was the highest between all the 2 adjacent developmental stages (N = 854) and, unlike the other comparator groups, most of them were down-regulated at the E8 stage (N = 803) (Figure 1E). This suggested that the dorsal skin transcriptome of the black-boned chickens underwent a dramatic shift at this stage, and that the developmental process from E7 to E8 was a critical turning point for skin melanosis.

Landscape of Gene Dynamic Expression in 10 Skin Developmental Stages

We observed successive changes in the dorsal skin of black-boned chickens from E4 to E13. From E8, the dorsal skin darkened significantly and, at E9, feather follicles began to appear (Figure 2A). Therefore, to study the transcriptome dynamics during skin development, we applied the fuzzy c-means algorithm to cluster the gene expression profiles at 10 stages. Overall, we observed 9 different temporal pattern clusters that represented genes that were regulated differently. The genes in cluster 1 showed a rapid decrease in expression from E7 to E8. GO analysis shows that these genes were associated primarily with intercellular signaling, and they were enriched with terms related to synaptic membranes, gated channel activity, and modulation of chemical synaptic transmission (Figure 2B). This may have involved the origin and differentiation of melanocytes in the early embryo. These genes may have an important influence on the formation and function of skin cells.

The genes in clusters 2 and 3 showed similar expression patterns, and both reached maximum expression at E12. Cluster 2 was enriched with terms related to aerobic respiration, mitochondrial transport, and the ribose phosphate biosynthesis process, which may be related to energy metabolism and proliferation and differentiation of melanocytes during melanin pigmentation

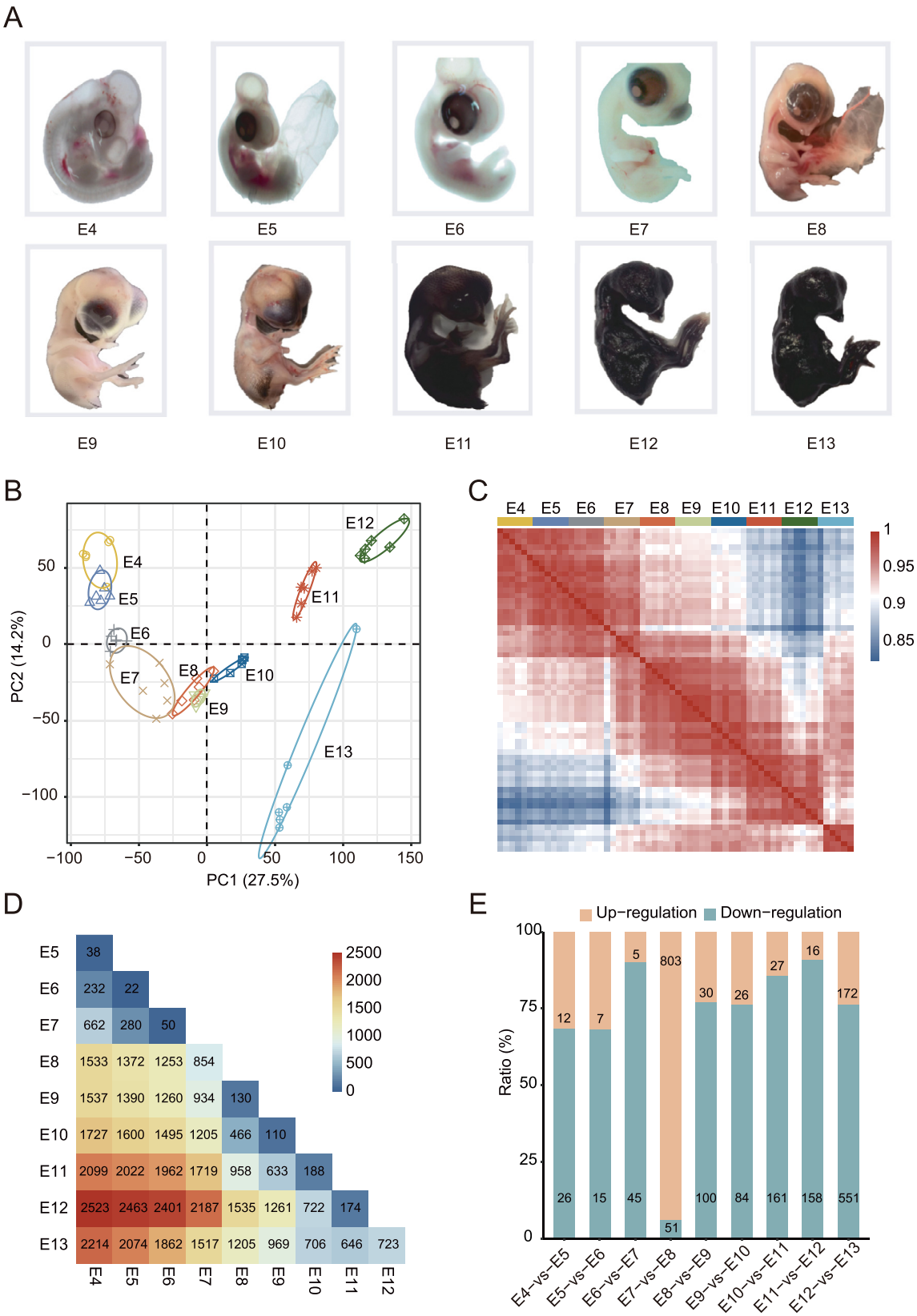

Figure 1. The comprehensive overview of the transcriptome of Panjiang black-bone chickens. (A) Whole-body photographs of chick embryos at embryonic stage from d 4 to d 13 of incubation, which show morphological changes throughout development. (B) PCA analysis based on the TPM values of genes from the RNA-seq samples; the ellipse encompasses the samples of each respective group. (C) Spearman correlation heatmap that shows the correlation between each RNA-seq sample. The color spectrum ranges from blue, which indicates a low correlation, to red, which signifies a high correlation. (D) Heatmap of the number of pairwise comparisons of DEG in skin samples from 10 time periods. (E) Bar plots that show the proportion of differentially up-regulated (orange) and down-regulated (blue) genes to the total number of DEGs in skin samples from each of 2 adjacent periods (9 comparison groups in total). The exact numbers are also labelled in the corresponding positions in the plot. Differential up- or down-regulation represents genes that were highly expressed in the earlier or later of the 2 adjacent periods.

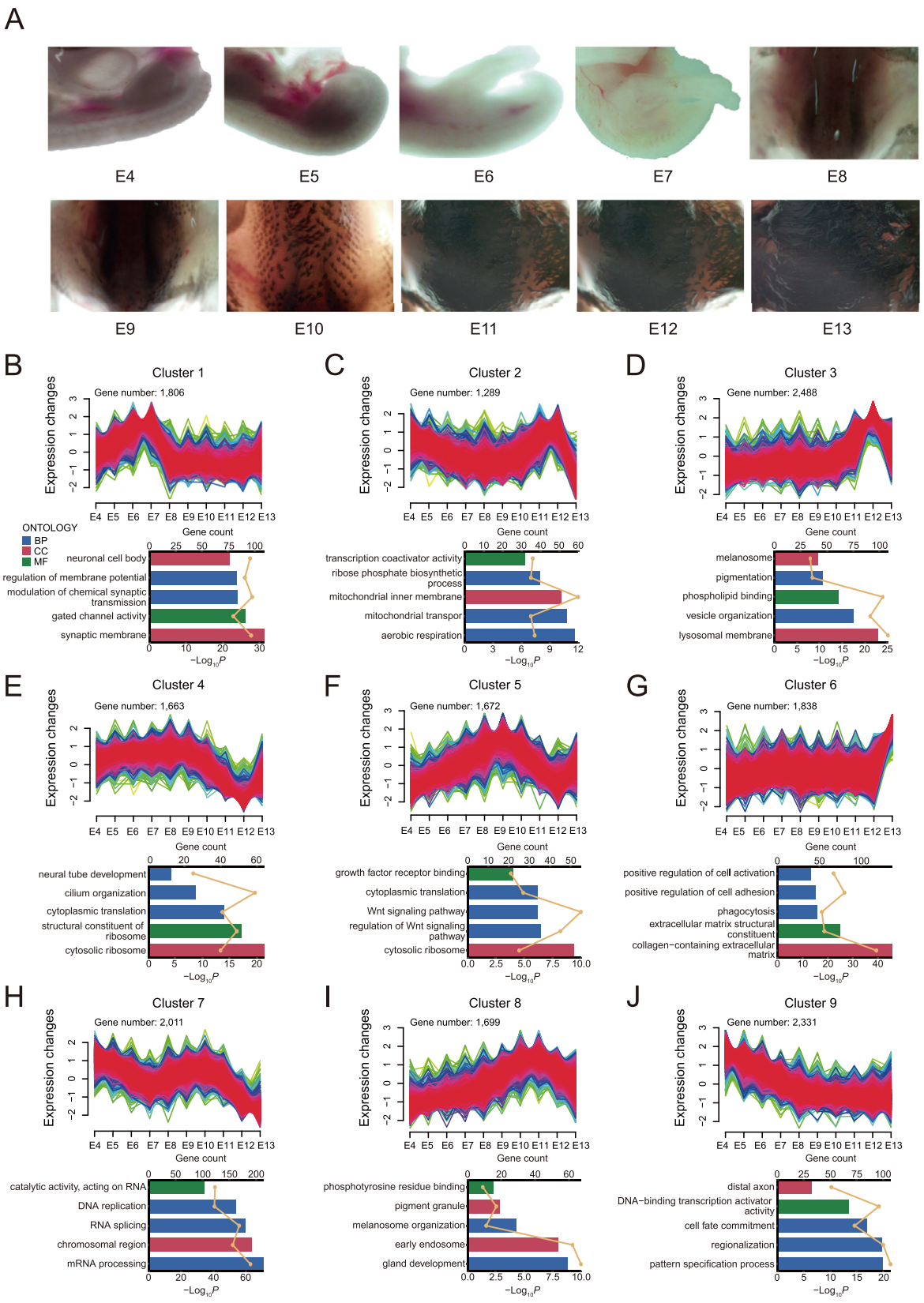

Figure 2. Dynamic gene expression landscapes of Panjiang black-bone chickens. (A) Close-up photograph of the dorsal skin of a chick embryo at embryonic stage from d 4 to d 13 of incubation, which shows the process of melanin pigmentation in the dorsal skin throughout development. (B–J) Clustering of fuzzy c-means of 9 distinct temporal patterns of gene expressions. The x-axis represents 10 developmental time points, and the y-axis represents TPM values of genes after standardization. The bar plot below shows the GO terms for each cluster. The different colors represent the 3 types of GO, biological processes (red), cellular components (blue), and molecular functions (green). The upper axis corresponds to the line plot and represents the number of genes, and the lower axis corresponds to the bar plot and represents the *P*-value.

(Figure 2C). Cluster 3 was enriched with many terms related to membrane and vesicular organization and with pigmentation and melanosome terms related directly to melanin synthesis and transport (Figure 2D). This suggested that at this stage melanin was synthesized in large quantities and transported to keratinocytes.

Genes in clusters 4 and 5 also showed a similar expression pattern; their expression increased gradually in the early phase to reach a maximum at E8 to E9, and then it decreased gradually to reach a minimum at E12. In both clusters, there was an enrichment in terms related to cytoplasmic ribosomes and cytoplasmic translation, which may be associated with the synthesis of some important proteins, such as transport proteins and enzymes (Figures 2E−F). Cluster 5 was also enriched for the Wnt signaling pathway, which plays an important role in melanin pigmentation (Figure 2F). The expression of genes in cluster 6 was up-regulated progressively throughout the developmental stages and enriched to the extracellular matrix, which not only provided cell support and structural scaffolding, but also participated in cellular interactions and signal transduction through collagen (Figure 2G).

The expression of genes in clusters 7 and 9 was gradually down-regulated throughout the developmental stages. Cluster 7 was enriched for mRNA processing, RNA splicing, and DNA replication (Figure 2H). Cluster 9 was enriched for pattern specification processes, regionalization, and cell fate commitment (Figure 2J). This was consistent with the dynamic nature of embryonic development. Expression of genes in cluster 8 increased gradually to a maximum around E11, and it was enriched in terms related to gland development, early endosomes, melanosome organization, and binding of phosphotyrosine residue (Figure 2I). This was similar to cluster 3 and demonstrated that melanin was synthesized in large quantities during this stage.

Key Stages in The Process of Skin Melanin Pigmentation

During the development of E7 to E8, the dorsal skin of the black-bone chicken suddenly darkened significantly (Figure 2A). To validate this observation and explore key pathways in the melanin pigmentation process, we performed a GSEA analysis using all differentially expressed genes between 2 adjacent developmental stages and showed the pathways that ranked in the top 10 for standardized enrichment scores (NES). During development from E4 to E6, terms related to the extracellular matrix were upregulated progressively (Figure 3A and Supplementary Figure S2A). This provided the necessary support and guidance for the localization, migration, proliferation, and differentiation of melanocytes in the skin during early embryonic development.

In addition, some extracellular matrix components influenced melanocyte function by regulating cell signaling pathways or by providing growth factors. During the development from E6 to E7, terms related to melanin biosynthesis and melanin metabolism were upregulated significantly (Figure 3B). E7 may be the key stage of mass synthesis and metabolism of melanin. During the development from E7 to E8, small ribosome subunits, keratin fibers, and keratinization terms were upregulated significantly (Figure 3C). This began at E8 and continued through to E12. Terms related to epidermal development, keratinocyte differentiation, melanosome membranes, and lysosomal membranes showed a continued upward trend (Supplementary Figures S2B−E). This indicated that during this stage, melanin was synthesized continuously and transferred to keratinocytes in large quantities, thus giving the skin a black appearance. During the development from E12 to E13, many terms related to the extracellular matrix were again upregulated significantly (Supplementary Figure S2F). After E13, various melanin synthesis and transport processes in the dorsal skin stabilized.

In addition, to investigate which genes played a key role in the initiation of melanin synthesis from E6 to E7, we visualized the melanogenesis pathway and showed key genes in that pathway (Figure 3D). Genes with differentially high expression in the E6 phase were concentrated mainly in the upstream of the melanogenesis pathway, and they were involved mainly in the preparation of early substances during the synthesis of melanin. In the E7 phase, many genes related to the melanogenesis pathway were overexpressed differentially, especially during melamine synthesis and tyrosine metabolism.

Network Analysis of Melanin Pigmentation Based on Weighted Gene Co-Expression Network Analysis

In addition, we used weighted gene co-expression network analysis (**WGCNA**) to analyze the network of key genes in the melanin pigmentation process. The analysis yielded 15 modules (Figures 4A and B). Further, we calculated Spearman correlation coefficients between each module and each sampling stage. The correlation coefficients between the expression of the genes in the blue module and the different sampling stages showed a tendency to increase with skin development (E4−E12) (Figure 4B), which was consistent with clusters 3 and 8 (Figure 2). The expression of genes in the blue module showed an increase during the E4 to E12 stages (Figure 4C). GO enrichment analysis of genes in the blue module showed that 5 of the 10 most significant terms were associated with epidermal development and melanin pigmentation (Supplementary Table S2). Therefore, the blue module was a melanin pigmentation-related module.

Genes with Module Membership (**MM**) values over 0.93 in the blue module were used to perform gene network analysis (Supplementary Table S3). *MITF, SLC24A5, MLPH, RAB32, KIT, RAB27A, DCT, TYRP1, TYR, OCA2, PMEL, CDH3, and GPR143* were involved in pigmentation function. Among them,

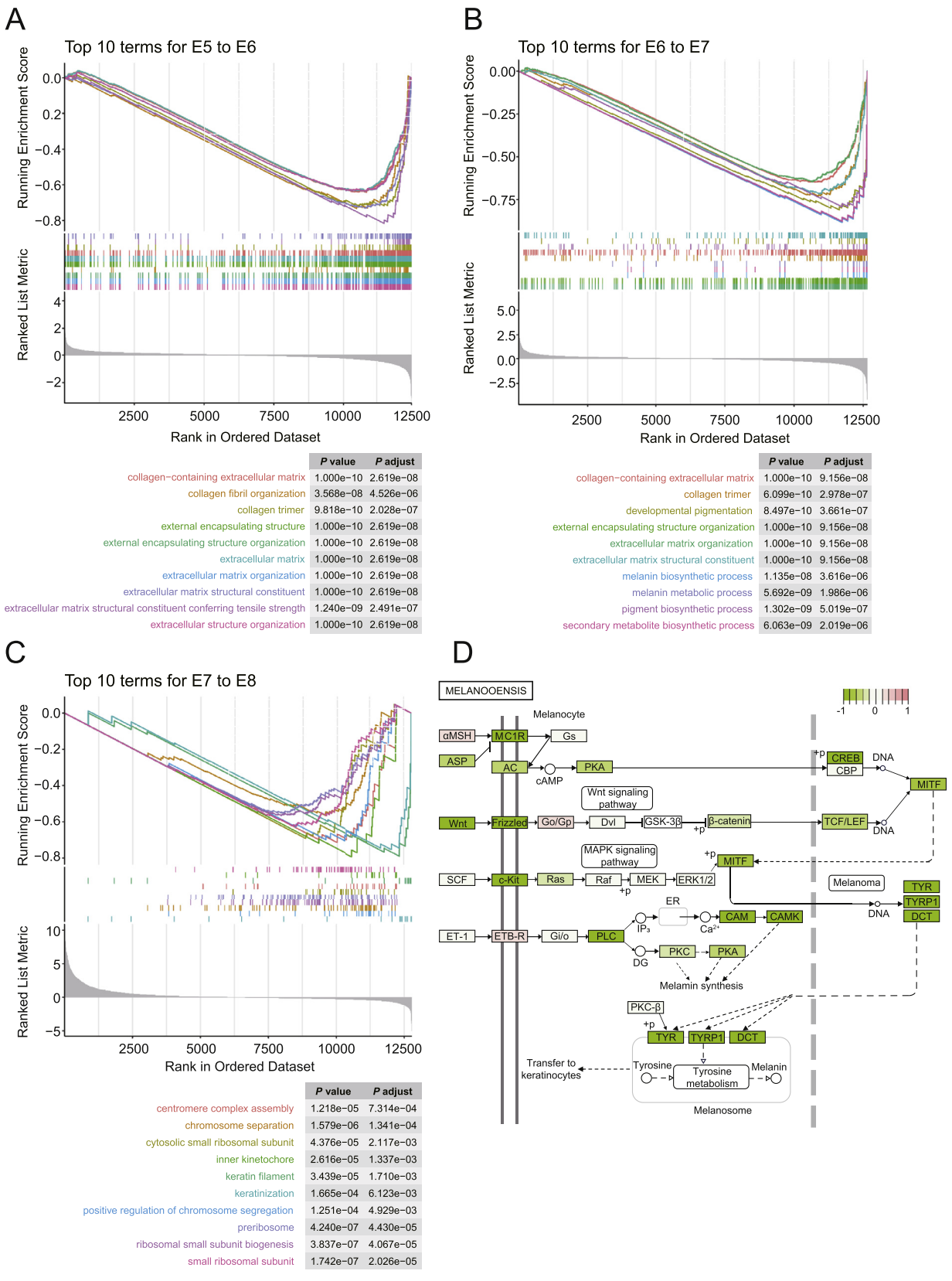

	P value	*P* adjust
collagen−containing extracellular matrix	1.000e−10	2.619e−08
collagen fibril organization	3.568e−08	4.526e−06
collagen trimer	9.818e−10	2.028e−07
external encapsulating structure	1.000e−10	2.619e−08
external encapsulating structure organization	1.000e−10	2.619e−08
extracellular matrix	1.000e−10	2.619e−08
extracellular matrix organization	1.000e−10	2.619e−08
extracellular matrix structural constituent	1.000e−10	2.619e−08
extracellular matrix structural constituent conferring tensile strength	1.240e−09	2.491e−07
extracellular structure organization	1.000e−10	2.619e−08

	P value	*P* adjust
collagen−containing extracellular matrix	1.000e−10	9.156e−08
collagen trimer	6.099e−10	2.978e−07
developmental pigmentation	8.497e−10	3.661e−07
external encapsulating structure organization	1.000e−10	9.156e−08
extracellular matrix organization	1.000e−10	9.156e−08
extracellular matrix structural constituent	1.000e−10	9.156e−08
melanin biosynthetic process	1.135e−08	3.616e−06
melanin metabolic process	5.692e−09	1.986e−06
pigment biosynthetic process	1.302e−09	5.019e−07
secondary metabolite biosynthetic process	6.063e−09	2.019e−06

	P value	*P* adjust
centromere complex assembly	1.218e−05	7.314e−04
chromosome separation	1.579e−06	1.341e−04
cytosolic small ribosomal subunit	4.376e−05	2.117e−03
inner kinetochore	2.616e−05	1.337e−03
keratin filament	3.439e−05	1.710e−03
keratinization	1.665e−04	6.123e−03
positive regulation of chromosome segregation	1.251e−04	4.929e−03
preribosome	4.240e−07	4.430e−05
ribosomal small subunit biogenesis	3.837e−07	4.067e−05
small ribosomal subunit	1.742e−07	2.026e−05

Figure 3. Initiation of melanin pigmentation of Panjiang black-bone chickens. (A−C) The GSEA plot shows the top 10 enrichment analyses between 2 adjacent time periods. Different colors correspond to different terms. The table in the upper right corner shows the *P*-value and corrected *P*-value for each term. (D) KEGG pathway plot that demonstrates the melanogenesis pathway enriched between E6 and E7. Color shades represent $\log_2$ fold change values, red represents up-regulation in E6, and green represents up-regulation in E7.

DCT, TYR, and *TYRP1* were all involved in the melanosome and melanin biosynthetic process. *PRKCH, DSG4, SCEL, KRT17, PPL, KRT16, SFN, PKP1, KRT14, KRT5, CDH3, JUP, CERS3, ASAH1, CLDN1, EVPL, DSP, GRHL2,* and *FA2H* were involved in epidermal cell differentiation, and there were interactions

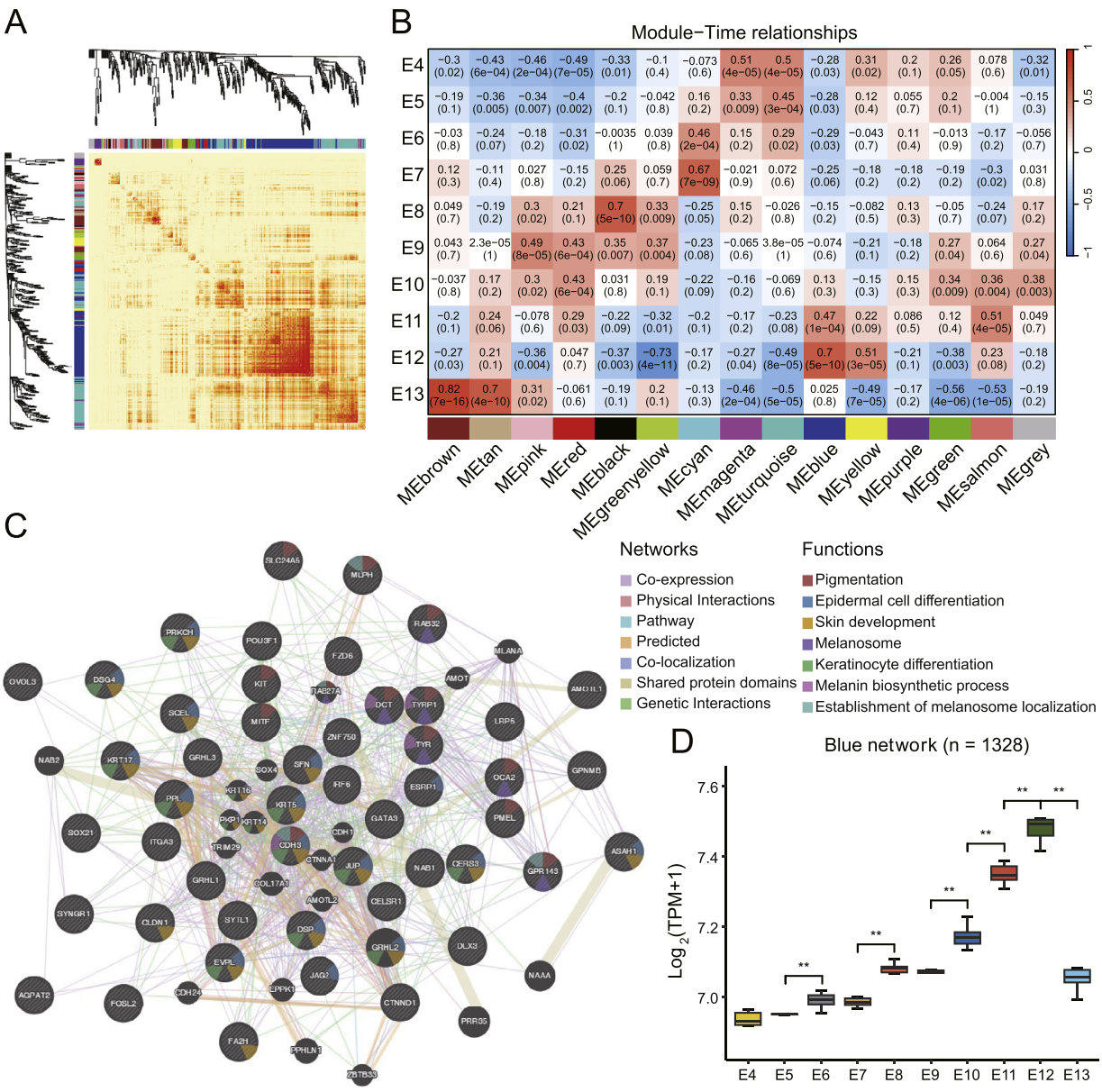

Figure 4. Weighted gene co-expression network analysis (**WGCNA**) of Panjiang black-bone chickens. (A) Heatmap that depicts the topological overlap matrix among all genes in the analysis. Blocks of darker colors along the diagonal indicate 15 modules. (B) Heatmap that shows module −time points correlation. (C) The correlation networks of major genes from the blue modules. The colors of the lines represent different types of linkage. The size of the circles represents the importance of the gene nodes, and the different colored blocks represent different functions enriched. (D) Box plots that show expression pattern of the blue module gene network. The x-axis indicates 10 time points, and gene expression data were normalized to Log_2(TPM+ 1). Asterisk is significantly different at $P < 0.05$ (Wilcoxon test).

between these genes and *MITF, KIT*, and *GRP143* (Figure 4D). These results suggested that *DCT, TYR,* and *TYRP1* were key functional genes for melanin synthesis in chicken epidermis and that there is a deep genetic interplay between melanin pigmentation and epidermal cell differentiation.

Differential Transcriptome Dynamics of Skin Melanin Pigmentation Between Black-Skinned Chickens and White-Skinned Chickens

To further compare the transcriptome differences in skin melanin pigmentation between black-bone chickens (black-skinned chickens) and other chicken breeds at the same embryonic developmental stages, we employed the same strategy to perform RNA-seq on the dorsal skin of white-skinned chickens (Youxin Ma chickens). A total of 1.4 billion paired-end reads (2 × 150 bp), equivalent to 417.95 Gb of sequencing data, were generated. The average mapping rate of clean RNA-seq reads to the reference genome (GRCg7b) was 95.71% (Supplementary Table S4). These results indicated that the sequencing data had a high quality of comparison.

The results of PCA analysis showed that the 60 samples were clustered separately according to different developmental stages, with a trend of continuous temporal distribution (Supplementary Figure S3A). Starting from E8 to E9, the Spearman correlation between

samples from different developmental stages noticeably decreases (Supplementary Figure S3B). In addition, the number of DEG between stages E8 and E9 significantly increases in white-skinned chickens (N = 1317), which is later than in black-skinned chickens (Supplementary Figure S3C). Interestingly, unlike the other comparator groups, most of DEG are down-regulated at the E8 stage and continue into E9, similar to the results in black-skinned chickens (Supplementary Figure S3D). This indicates that both species conservation and breed heterogeneity exist between the black-bone chicken and the Youxin Ma chicken. Through DEG analysis, we can reveal the differences in molecular mechanisms involved in skin melanin pigmentation processes.

The DEG analysis at the same developmental stage revealed that black-skinned chickens and white-skinned chickens exhibit the greatest transcriptional differences at E8. Specifically, 596 genes were differentially highly expressed in black-skinned chickens, while 1092 genes showed differentially highly expressed in white-skinned chickens (Figure 5A and Supplementary Table S5). We then focused on the transcriptional changes of *DCT, TYR, TYRP1, MITF*, and *CDH3* during embryonic development in the 2 breeds (Figure 5B and Supplementary Figure S3E). We found that *DCT, TYR, TYRP1*, and *CDH3* are expressed at higher levels in black-skinned chickens at nearly all stages, whereas the expression of *MITF* shows little difference. This indicates that there are greater differences in melanin synthesis and transport processes between black-skinned and white-skinned chickens. Additionally, the expression levels of these genes in black-skinned chickens sharply increased from E6, whereas in white-skinned chickens, this phenomenon occurred after E8. This suggests that melanin pigmentation in the skin occurs at an earlier stage in black-skinned chickens compared to white-skinned chickens.

Finally, we performed GO enrichment analysis on the significant DEGs (adjusted P-value < 0.01 and absolute value of log2FoldChange > 2) identified from these comparisons. In black-skinned chickens, starting from E6, terms related to melanin synthesis, metabolism, epidermal cell development, and differentiation were significantly enriched (Figure 5C). These terms were enriched only at E4 in white-skinned chickens, and from E8 onwards, most enriched terms were associated with muscle development, extracellular matrix, and cell fate (Figure 5D). This indicates that melanin synthesis and transfer in black-skinned chickens initiate on a large scale from E6 onwards, showing significant differences compared to white-skinned chickens.

DISCUSSION

Skin melanin pigmentation has many important physiological and pathological implications that are related to camouflage, mimicry, social communication, inflammation, and protection against harmful effects of solar radiation (Li et al., 2022; Slominski et al., 2004). This biological process continues from the embryonic stage (Cui et al., 2023; Li et al., 2020). However, transcriptional changes of skin melanin pigmentation during embryonic developmental stages have not been explored. In this study, although influenced by possible individual differences, we found that skin melanin pigmentation was a dynamically changing process in which multiple pathways were involved collectively over 10 developmental time points from E4 onwards. Our study revealed the diversity and complexity of this biological process. By studying melanin pigmentation in the embryonic skin of black-bone chickens, we not only deepened our understanding of the physiological mechanisms in chickens, but we also provide an opportunity to extend these insights to other species, which should lead to a broader understanding of the universal regulation and physiological mechanisms of skin melanin pigmentation.

During early embryonic development, neural crest cells that arise from the neuroectoderm are highly motile (Li, et al., 2020). Through embryonic migration and lineage specification, they delaminate and differentiate into melanoblasts, peripheral and enteric neurons, and glial precursor cells (Huang et al., 2004; Soldatov et al., 2019). This involves a complex process of coordinated multiple chemical and mechanical signals (Piacentino et al., 2020; Shellard et al., 2019). Subsequently, melanoblasts migrate through the dermis to the dorsolateral epidermis (Vandamme et al., 2019). They use long actin/microtubule-based pseudopods and short actin-based protrusions to navigate through the epidermal keratinocyte layer (Li et al., 2011). Furthermore, the efficiency of melanoblast migration is related to the precise coordination of integrin-mediated, cell-extracellular matrix (**ECM**) adhesion (Haage et al., 2020).

In mice, melanoblasts migrated from the dermis to the epidermal compartment starting from E10.5, and colonization was completed by E15.5 (Baxter et al., 2003; Hirobe 1984; Luciani et al., 2011). In ducks, the migration process is basically complete at E13 because mRNA expression levels of most melanin synthesis-related genes are highest at this stage (Xi et al., 2020). Our black-bone chicken data showed a high concentration of myofibrillar and ECM related terms at E4 to E6 stages, which suggested that melanoblasts migrated to the epidermis from E4 or earlier. The expression level of melanin synthesis-related genes reached a peak at E12, which indicated that melanocyte migration was completed at E12. This is also similar to earlier results obtained by antibody staining (Erickson et al., 1992). This proves that this series of biological processes is highly conserved in vertebrates. The difference in time may be due to factors, such as genetic information, geographical location, and incubation conditions.

Melanoblasts differentiate further into melanocytes and melanocyte stem cells (Petit et al., 2016). Like neurons, melanocytes form highly polarized dendrites after homing to the epidermis or hair follicle (Li et al., 2020). This morphology enables them to establish contact with neighboring keratinocytes and to gain the ability to

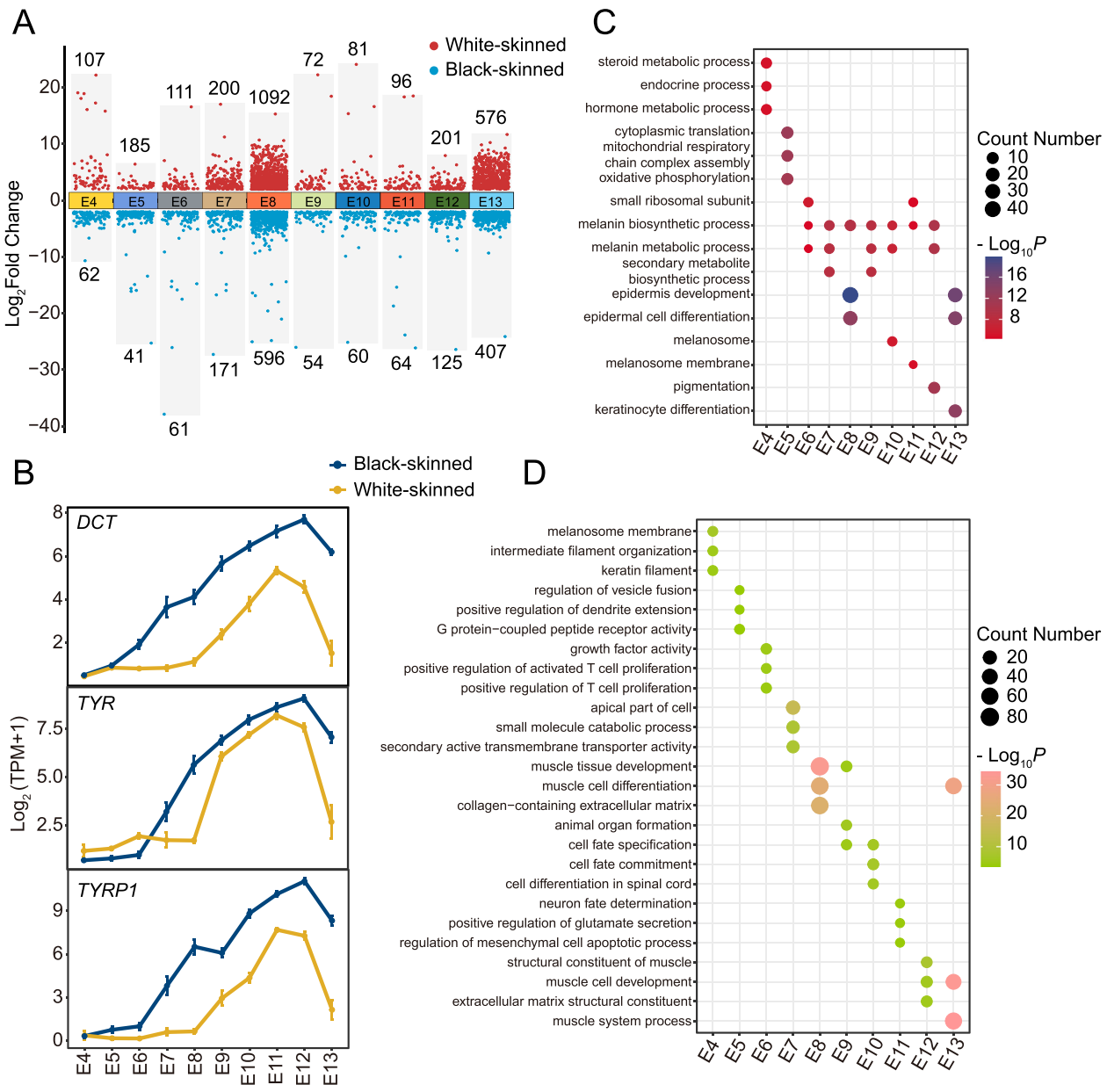

Figure 5. Transcriptome differential analysis between black-skinned and white-skinned chickens. (A) Multiple volcano plots showing DEG in the dorsal skin of Panjiang black-skinned chickens (blue) and white-skinned chickens (red) at each embryonic stages. Digital display number of DEG. (B) Line plots that show expression patterns of genes involved in skin melanin pigmentation. The x-axis indicates 10 time points, and gene expression data were normalized to Log_2(TPM+ 1). The vertical line on each point indicates the standard error. (C−D) Dot plots showing the GO enrichment analysis of significant DEGs in Panjiang black-skinned chickens (C) and white-skinned chickens (D) at each embryonic stage. Color indicates *P*-value and circle indicates genes counts.

produce melanin and to release melanin-containing melanosomes (Vandamme et al., 2019). During the development of E7 to E8 in black-bone chickens, the expression of many genes related to synapses and pattern-specification terms was down-regulated. This stage may be key for the fate determination and differentiation of neural crest cells to form various skin cells that include melanocytes. This may also be one of the reasons for the sudden increase in the amount of DEG at this stage. After that, energy metabolism, ribosome synthesis, DNA and RNA processing and synthesis provide the basic material support for the whole synthesis process of melanin (Allouche et al., 2021; Bajpai et al., 2023; Tian et al., 2021).

Melanosomes share proteins with lysosomes and are acidic in their early stages (Delevoye et al., 2019). Its biogenesis is divided into 4 organelle stages that range from early and nonpigmented (stage I-II) to late and pigmented (stage III-IV) (Tian et al., 2021). Pigmentation occurs when melanin synthesizes melanosomes in lysosomal-like structures called melanosomes and then transfers these melanosomes to keratinocytes (Raposo et al., 2007). Our data show that melanin synthesis-related pathways were up-regulated significantly during E6 to E7, but no darkening of the dorsal skin was observed, which suggested that this phase was phase I-II of melanosome biogenesis. Related terms such as keratosis were upregulated significantly during E7-E8, and the apparent darkening of the dorsal skin was observed under the anatomical microscope, which suggested that this stage was in the III-IV stage of melanosome biogenesis.

In addition, in previous studies, 4 possible models for the transfer of melanosomes from melanocytes to keratinocytes were summarized (Tadokoro et al., 2017; Wu et al., 2014). Our transcriptome data support the theory that melanosomes were secreted by melanocytes and then internalized by keratinocytes (Moreiras et al., 2021); during development to E12 and accompanied by the transfer of melanosomes, a series of genes related to endosomal and vesicle tissue were up-regulated gradually. During the growth from E10 to E11, which marks the peak period of melanosome transfer to the epidermis and feather keratinocytes, the black-bone chicken embryo exhibits rapid feather growth and blackening on its body surface. In summary, our results suggested that melanin synthesis-related pathways were up-regulated at an early stage during embryonic development in black-bone chickens, but true skin melanin pigmentation occurred at subsequent stages, which corresponded to different stages of melanosome biogenesis. This discovery contributes to a deeper understanding of the molecular mechanism and timing of melanin formation in black bone chicken skin.

Skin melanin pigmentation is a process regulated precisely by a series of genes and transcription factors. Through WGCNA analysis, we identified core factors that were involved in different key pathways to perform different functions. Enzymes, such as *DCT, TYR,* and *TYRP1*, were the key factors in melanin synthesis of melanosomes that initiated tyrosine to produce dopa quinone, which is the precursor of eumelanin and phaeomelanin, through oxidation and other processes (Centeno et al., 2023; Raposo et al., 2007). *MITF*, which was the main transcription factor that regulated this process, was embedded in the transcriptional network that controlled the development of neural crest melanocytes (Baxter et al., 2010). Studies in mice and fish have shown that melanocyte-specific organelles (melanosomes) that encoded melanocytes and melanin synthesis pathways were affected when *MITF* expression was lacking (Béjar et al., 2003; Steingrímsson et al., 2004).

Our results showed that the expression of these key genes arose sharply from E7 and then continued to rise until E12 reached its maximum. In addition, the transfer of melanin from melanocytes to keratinocytes was influenced by calcium flux regulation (Carsberg et al., 1995; Zhang et al., 2022a). *CDH3* encoded an intercellular adhesion molecule (P-cadherin) that belongs to the cadherin superfamily, and its expression was up-regulated gradually with the increase in the concentration of intracellular calcium ions (Furukawa et al., 1997; Polisetti et al., 2022). *CDH3* plays an important role in cell differentiation, migration, and intercellular adhesion (Bauer et al., 2012; Le Borgne-Rochet et al., 2019; Nishimura et al., 1999; Van Marck et al., 2005). Interestingly, both the synthesis of melanin and the transfer of melanin to keratinocytes requires extensive involvement of these processes (Cui et al., 2023; Moreiras et al., 2021). In the gene network we constructed, *CDH3* was a core factor involved in a variety of biological processes, which included pigmentation, keratinocyte differentiation, and melanin synthesis. Therefore, we speculate that *CDH3* was a key factor in skin melanin pigmentation during embryonic development. Of course, more research is needed to confirm this further.

In black-bone chickens, which have black skin, muscles, bones, and internal organs are all heavily pigmented with melanin, resulting in their distinctive black skin and black meat due to the extensive distribution of melanocytes throughout their bodies (Nganvongpanit et al., 2020; Zi et al., 2023). In contrast, in white-skinned chickens, melanin pigmentation is primarily limited to the feathers, with the skin and meat generally appearing pink or white. Therefore, there are significant differences in the melanin pigmentation processes between these 2 types of chickens. Khumpeerawat et al. used qRT-PCR to analyze the expression differences of skin color-related genes among various chicken breeds (Khumpeerawat et al., 2021). They found that compared to chickens with light black or yellowish-white skin, chickens with black skin exhibited higher expression levels of *TYRP1* and *TYR* genes. However, compared to other skin colors, chickens with yellowish-white skin showed higher expression of the *ASIP* gene. Wang et al. performed single-cell RNA sequencing on the skin of 3-mo-old black-feathered and white-feathered chickens, revealing 2 subpopulations of keratinocytes and melanocytes with higher abundance in black-feathered chickens (Wang et al., 2024). In this study, we extended previous research by discovering that in black-bone chickens, melanin pigmentation and transfer activities start to increase significantly from E6 and continue to rise. In contrast, in white-skinned chickens, these biological processes begin at E8 and are significantly less active compared to black-bone chickens. The main differences lie in the expression of genes related to melanin synthesis and transfer, such as *DCT, TYR, TYRP1*, and *CDH3*. These results provide data to support the explanation of skin color differences between black-bone chickens and white-skinned chickens from a developmental perspective and reveal the key roles of these genes in the process of skin color formation.

CONCLUSIONS

In summary, we present evidence here that skin melanin pigmentation in black-bone chickens involved a sequence of biological processes and was regulated precisely by many genes and transcription factors. Melanoblasts migrated from E4 to the epidermis consistently until E12. From E6 onwards, melanin was synthesized in large amounts and transferred to the epidermis cells and feather follicles, and genes such as *DCT, TYR, TYRP1,* and *MITF* played a key role in this process, which is significantly different from that of white-skinned chickens. E7∼E8 was a key stage for melanocytes to form dendritic forms and to transfer melanin to keratinocytes. This transfer process may be accomplished through exocytosis and internalization. In addition, *CDH3*, which was a core factor involved in a

variety of biological processes, may have important implications for skin melanin pigmentation, although more research is needed to verify further.

ACKNOWLEDGMENTS

This work was supported by STI 2030-Major Projects (2023ZD04069), National Key R&D Program of China (Grant No. 2021YFD1300100), programs ([2022]097, and [2022]099) from Science and Technology Department of Guizhou Province, "JBGS" Project of Seed Industry Revitalization in Jiangsu Province (JBGS [2021]109), and Guangxi Key R&D Program (No. AB21220005).

Author contributions: The original idea for this study was conceived by Diyan Li and Chungang Feng. Tao Wang, Diyan Li, and Chungang Feng designed the experimental methods. Dong Leng, Zhiying Huang, Maosen Yang, Mengmeng Li, Jia Liu, and Xiaomeng Miao collected materials. Dong Leng and Maosen Yang analyzed the data. The manuscript was written by Dong Leng. Finally, all the authors read and approved the final manuscript.

DISCLOSURES

The authors declare that they have no known competing financial interests or personal relationships that could have appeared to influence the work reported in this paper.

SUPPLEMENTARY MATERIALS

Supplementary material associated with this article can be found in the online version at doi:10.1016/j.psj.2024.104210.

REFERENCES

Allouche, J., I. Rachmin, K. Adhikari, L. M. Pardo, J. H. Lee, A. M. McConnell, S. Kato, S. Fan, A. Kawakami, Y. Suita, K. Wakamatsu, V. Igras, J. Zhang, P. P. Navarro, C. M. Lugo, H. R. Noonan, K. A. Christie, K. Itin, N. Mujahid, J. A. Lo, C. H. Won, C. L. Evans, Q. Y. Weng, H. Wang, S. Osseiran, A. Lovas, I. Németh, A. Cozzio, A. A. Navarini, J. J. Hsiao, N. Nguyen, L. V. Kemény, O. Iliopoulos, C. Berking, T. Ruzicka, R. Gonzalez-José, M. C. Bortolini, S. Canizales-Quinteros, V. Acuna-Alonso, C. Gallo, G. Poletti, G. Bedoya, F. Rothhammer, S. Ito, M. V. Schiaffino, L. H. Chao, B. P. Kleinstiver, S. Tishkoff, L. I. Zon, T. Nijsten, A. Ruiz-Linares, D. E. Fisher, and E. Roider. 2021. NNT mediates redox-dependent pigmentation via a UVB- and MITF-independent mechanism. Cell 184:4268–4283. e20.

Bajpai, V. K., T. Swigut, J. Mohammed, S. Naqvi, M. Arreola, J. Tycko, T. C. Kim, J. K. Pritchard, M. C. Bassik, and J. Wysocka. 2023. A genome-wide genetic screen uncovers determinants of human pigmentation. Science 381:eade6289.

Bauer, K., M. Gosau, A. Bosserhoff, T. Reichert, and R. Bauer. 2012. P-cadherin controls the differentiation of oral keratinocytes by regulating cytokeratin 1/10 expression via C/EBP-beta-mediated signaling. Differentiation 84:345–354.

Baxter, L. L., R. T. Moreland, A. D. Nguyen, T. G. Wolfsberg, and W. J. Pavan. 2010. A curated online resource for SOX10 and pigment cell molecular genetic pathways. Database (Oxford) 2010: baq025.

Baxter, L. L., and W. J. Pavan. 2003. Pmel17 expression is Mitf-dependent and reveals cranial melanoblast migration during murine development. Gene. Expr. Pattern. 3:703–707.

Béjar, J., Y. Hong, and M. Schartl. 2003. Mitf expression is sufficient to direct differentiation of medaka blastula derived stem cells to melanocytes. Development 130:6545–6553.

Braasch, I., M. Schartl, and J. N. Volff. 2007. Evolution of pigment synthesis pathways by gene and genome duplication in fish. BMC Evol. Biol. 7:74.

Bray, N. L., H. Pimentel, P. Melsted, and L. Pachter. 2016. Near-optimal probabilistic RNA-seq quantification. Nat. Biotechnol. 34:525–527.

Carsberg, C. J., K. T. Jones, G. R. Sharpe, and P. S. Friedmann. 1995. Intracellular calcium modulates the responses of human melanocytes to melanogenic stimuli. J. Dermatol. Sci. 9:157–164.

Centeno, P. P., V. Pavet, and R. Marais. 2023. The journey from melanocytes to melanoma. Nat. Rev. Cancer. 23:372–390.

Christiansen, J. H., E. G. Coles, and D. G. Wilkinson. 2000. Molecular control of neural crest formation, migration and differentiation. Curr. Opin. Cell. Biol. 12:719–724.

Cui, Y. Z., and X. Y. Man. 2023. Biology of melanocytes in mammals. Front. Cell. Dev. Biol. 11:1309557.

Delevoye, C., M. S. Marks, and G. Raposo. 2019. Lysosome-related organelles as functional adaptations of the endolysosomal system. Curr. Opin. Cell. Biol. 59:147–158.

Dobin, A., C. A. Davis, F. Schlesinger, J. Drenkow, C. Zaleski, S. Jha, P. Batut, M. Chaisson, and T. R. Gingeras. 2013. STAR: Ultrafast universal RNA-seq aligner. Bioinformatics 29:15–21.

Domingues, L., I. Hurbain, F. Gilles-Marsens, J. Sirés-Campos, N. André, M. Dewulf, M. Romao, C. Viaris de Lesegno, A. S. Macé, C. Blouin, C. Guéré, K. Vié, G. Raposo, C. Lamaze, and C. Delevoye. 2020. Coupling of melanocyte signaling and mechanics by caveolae is required for human skin pigmentation. Nat. Commun. 11:2988.

Dorshorst, B., A. M. Molin, C. J. Rubin, A. M. Johansson, L. Strömstedt, M. H. Pham, C. F. Chen, F. Hallböök, C. Ashwell, and L. Andersson. 2011. A complex genomic rearrangement involving the endothelin 3 locus causes dermal hyperpigmentation in the chicken. PLoS Genet. 7:e1002412.

Erickson, C. A., T. D. Duong, and K. W. Tosney. 1992. Descriptive and experimental analysis of the dispersion of neural crest cells along the dorsolateral path and their entry into ectoderm in the chick embryo. Dev. Biol. 151:251–272.

Faraco, C. D., S. A. Vaz, M. V. Pástor, and C. A. Erickson. 2001. Hyperpigmentation in the Silkie fowl correlates with abnormal migration of fate-restricted melanoblasts and loss of environmental barrier molecules. Dev. Dyn. 220:212–225.

Furukawa, F., K. Fujii, Y. Horiguchi, N. Matsuyoshi, M. Fujita, K. Toda, S. Imamura, H. Wakita, S. Shirahama, and M. Takigawa. 1997. Roles of E- and P-cadherin in the human skin. Microsc. Res. Tech. 38:343–352.

Gammill, L. S., and M. Bronner-Fraser. 2003. Neural crest specification: migrating into genomics. Nat. Rev. Neurosci. 4:795–805.

Haage, A., K. Wagner, W. Deng, B. Venkatesh, C. Mitchell, K. Goodwin, A. Bogutz, L. Lefebvre, C. D. Van Raamsdonk, and G. Tanentzapf. 2020. Precise coordination of cell-ECM adhesion is essential for efficient melanoblast migration during development. Development 147:dev184234.

Hirobe, T. 1984. Histochemical survey of the distribution of the epidermal melanoblasts and melanocytes in the mouse during fetal and postnatal periods. Anat. Rec. 208:589–594.

Huang, X., and J. P. Saint-Jeannet. 2004. Induction of the neural crest and the opportunities of life on the edge. Dev. Biol. 275:1–11.

Khumpeerawat, P., M. Duangjinda, and Y. Phasuk. 2021. Factors affecting gene expression associated with the skin color of blackbone chicken in Thailand. Poult. Sci. 100:101440.

Le Borgne-Rochet, M., L. Angevin, E. Bazellières, L. Ordas, F. Comunale, E. V. Denisov, L. A. Tashireva, V. M. Perelmuter, I. Bièche, S. Vacher, C. Plutoni, M. Seveno, S. Bodin, and C. Gauthier-Rouvière. 2019. P-cadherin-induced decorin secretion is required for collagen fiber alignment and directional collective cell migration. J. Cell. Sci. 132:jcs233189.

Levy, C., M. Khaled, and D. E. Fisher. 2006. MITF: master regulator of melanocyte development and melanoma oncogene. Trends Mol. Med. 12:406–414.

Li, A., Y. Ma, X. Yu, R. L. Mort, C. R. Lindsay, D. Stevenson, D. Strathdee, R. H. Insall, J. Chernoff, S. B. Snapper, I. J. Jackson, L. Larue, O. J. Sansom, and L. M. Machesky. 2011. Rac1 drives melanoblast organization during mouse development by orchestrating pseudopod- driven motility and cell-cycle progression. Dev. Cell. 21:722–734.

Li, C., L. Kuai, R. Cui, and X. Miao. 2022. Melanogenesis and the targeted therapy of melanoma. Biomolecules 12:1874.

Li, D., T. Che, B. Chen, S. Tian, X. Zhou, G. Zhang, M. Li, U. Gaur, Y. Li, M. Luo, L. Zhang, Z. Xu, X. Zhao, H. Yin, Y. Wang, L. Jin, Q. Tang, H. Xu, M. Yang, R. Zhou, R. Li, Q. Zhu, and M. Li. 2017. Genomic data for 78 chickens from 14 populations. Gigascience 6:1–5.

Li, D., Y. Li, M. Li, T. Che, S. Tian, B. Chen, X. Zhou, G. Zhang, U. Gaur, M. Luo, K. Tian, M. He, S. He, Z. Xu, L. Jin, Q. Tang, Y. Dai, H. Xu, Y. Hu, X. Zhao, H. Yin, Y. Wang, R. Zhou, C. Yang, H. Du, X. Jiang, Q. Zhu, and M. Li. 2019. Population genomics identifies patterns of genetic diversity and selection in chicken. BMC Genom. 20 263-263.

Li, M., S. K. Knapp, and S. Iden. 2020. Mechanisms of melanocyte polarity and differentiation: What can we learn from other neuroectoderm-derived lineages? Curr. Opin. Cell. Biol. 67:99–108.

Lin, J. Y., and D. E. Fisher. 2007. Melanocyte biology and skin pigmentation. Nature 445:843–850.

Luciani, F., D. Champeval, A. Herbette, L. Denat, B. Aylaj, S. Martinozzi, R. Ballotti, R. Kemler, C. R. Goding, F. De Vuyst, L. Larue, and V. Delmas. 2011. Biological and mathematical modeling of melanocyte development. Development 138:3943–3954.

Moreiras, H., M. C. Seabra, and D. C. Barral. 2021. Melanin transfer in the epidermis: The pursuit of skin pigmentation control mechanisms. Int. J. Mol. Sci. 22:4466.

Mundy, N. I. 2005. A window on the genetics of evolution: MC1R and plumage colouration in birds. Proc. Biol. Sci. 272:1633–1640.

Muroya, S., R. Tanabe, I. Nakajima, and K. Chikuni. 2000. Molecular characteristics and site specific distribution of the pigment of the silky fowl. J. Vet. Med. Sci. 62:391–395.

Nganvongpanit, K., P. Kaewkumpai, V. Kochagul, K. Pringproa, V. Punyapornwithaya, and S. Mekchay. 2020. Distribution of melanin pigmentation in 33 organs of Thai black-bone chickens (Gallus gallus domesticus). Animals (Basel) 10:777.

Nishimura, E. K., H. Yoshida, T. Kunisada, and S.-I. Nishikawa. 1999. Regulation of E- and P-cadherin expression correlated with melanocyte migration and diversification. Development. Biol. 215:155–166.

Petit, V., and L. Larue. 2016. Any route for melanoblasts to colonize the skin!. Exp. Dermatol. 25:669–673.

Piacentino, M. L., Y. Li, and M. E. Bronner. 2020. Epithelial-to-mesenchymal transition and different migration strategies as viewed from the neural crest. Curr. Opin. Cell. Biol. 66:43–50.

Polisetti, N., L. Sharaf, G. Martin, G. Schlunck, and T. Reinhard. 2022. P-cadherin is expressed by epithelial progenitor cells and melanocytes in the human corneal limbus. Cells 11:1975.

Raposo, G., and M. S. Marks. 2007. Melanosomes—dark organelles Enlighten endosomal membrane transport. Nat. Rev. Mol. Cell. Biol. 8:786–797.

Robbins, L. S., J. H. Nadeau, K. R. Johnson, M. A. Kelly, L. Roselli-Rehfuss, E. Baack, K. G. Mountjoy, and R. D. Cone. 1993. Pigmentation phenotypes of variant extension locus alleles result from point mutations that alter MSH receptor function. Cell 72:827–834.

Shellard, A., and R. Mayor. 2019. Integrating chemical and mechanical signals in neural crest cell migration. Curr. Opin. Genet. Dev. 57:16–24.

Slominski, A., D. J. Tobin, S. Shibahara, and J. Wortsman. 2004. Melanin pigmentation in mammalian skin and its hormonal regulation. Physiol. Rev. 84:1155–1228.

Soldatov, R., M. Kaucka, M. E. Kastriti, J. Petersen, T. Chontorotzea, L. Englmaier, N. Akkuratova, Y. Yang, M. Häring, V. Dyachuk, C. Bock, M. Farlik, M. L. Piacentino, F. Boismoreau, M. M. Hilscher, C. Yokota, X. Qian, M. Nilsson, M. E. Bronner, L. Croci, W. Y. Hsiao, D. A. Guertin, J. F. Brunet, G. G. Consalez, P. Ernfors, K. Fried, P. V. Kharchenko, and I. Adameyko. 2019. Spatiotemporal structure of cell fate decisions in murine neural crest. Science 364:eaas9536.

Steingrímsson, E., H. Arnheiter, J. H. Hallsson, M. L. Lamoreux, N. G. Copeland, and N. A. Jenkins. 2003. Interallelic complementation at the mouse Mitf locus. Genetics 163:267–276.

Steingrímsson, E., N. G. Copeland, and N. A. Jenkins. 2004. Melanocytes and the microphthalmia transcription factor network. Annu. Rev. Genet. 38:365–411.

Tadokoro, R., and Y. Takahashi. 2017. Intercellular transfer of organelles during body pigmentation. Curr. Opin. Genet. Dev. 45:132–138.

Takeuchi, S., H. Suzuki, M. Yabuuchi, and S. Takahashi. 1996a. A possible involvement of melanocortin 1-receptor in regulating feather color pigmentation in the chicken. Biochim. Biophys. Acta. 1308:164–168.

Takeuchi, S., S. Suzuki, S. Hirose, M. Yabuuchi, C. Sato, H. Yamamoto, and S. Takahashi. 1996b. Molecular cloning and sequence analysis of the chick melanocortin 1-receptor gene. Biochim. Biophys. Acta. 1306:122–126.

Tian, X., Z. Cui, S. Liu, J. Zhou, and R. Cui. 2021. Melanosome transport and regulation in development and disease. Pharmacol. Ther. 219:107707.

Van Marck, V., C. Stove, K. Van Den Bossche, V. Stove, J. Paredes, Y. Vander Haeghen, and M. Bracke. 2005. P-cadherin promotes cell-cell adhesion and counteracts invasion in human melanoma. Cancer. Res. 65:8774–8783.

Vandamme, N., and G. Berx. 2019. From neural crest cells to melanocytes: cellular plasticity during development and beyond. Cell. Mol. Life Sci. 76:1919–1934.

Wang, L., Z. Xue, Y. Tian, W. Zeng, T. Zhang, and H. Lu. 2024. A single-cell transcriptome atlas of Lueyang black-bone chicken skin. Poult. Sci. 103:103513.

Wu, T., E. Hu, S. Xu, M. Chen, P. Guo, Z. Dai, T. Feng, L. Zhou, W. Tang, L. Zhan, X. Fu, S. Liu, X. Bo, and G. Yu. 2021. clusterProfiler 4.0: A universal enrichment tool for interpreting omics data. Innovation (Camb) 2:100141.

Wu, X., and J. A. Hammer. 2014. Melanosome transfer: it is best to give and receive. Curr. Opin. Cell Biol. 29:1–7.

Xi, Y., H. Liu, L. Li, Q. Xu, Y. Liu, L. Wang, S. Ma, J. Wang, L. Bai, R. Zhang, and C. Han. 2020. Transcriptome reveals multi pigmentation genes affecting dorsoventral pattern in avian body. Front. Cell. Dev. Biol. 8:560766.

Zhang, J., F. Liu, J. Cao, and X. Liu. 2015. Skin transcriptome profiles associated with skin color in chickens. PLoS One 10: e0127301.

Zhang, H., Z. Chen, A. Zhang, A. A. Gupte, and D. J. Hamilton. 2022a. The role of calcium signaling in melanoma. Int. J. Mol. Sci. 23:1010.

Zhang, P., Y. Cao, Y. Fu, H. Zhu, S. Xu, Y. Zhang, W. Li, G. Sun, R. Jiang, R. Han, H. Li, G. Li, Y. Tian, X. Liu, X. Kang, and D. Li. 2022b. Revealing the regulatory mechanism of lncRNA-LMEP on melanin deposition based on high-throughput sequencing in Xichuan chicken skin. Genes (Basel) 13:2143.

Zhu, W. Q., H. F. Li, J. Y. Wang, J. T. Shu, C. H. Zhu, W. T. Song, C. Song, G. G. Ji, and H. X. Liu. 2014. Molecular genetic diversity and maternal origin of Chinese black-bone chicken breeds. Genet. Mol. Res. 13:3275–3282.

Zi, X., X. Ge, Y. Zhu, Y. Liu, D. Sun, Z. Li, M. Liu, Z. You, B. Wang, J. Kang, T. Dou, C. Ge, and K. Wang. 2023. Transcriptome profile analysis identifies candidate genes for the melanin pigmentation of skin in Tengchong snow chickens. Vet. Sci. 10:341.